

Development of Control and Monitoring of BLDC Motor Speed without Sensor with Back Emf Detection

1st Nada Syadza Azizah
Electrical Engineering Dept.
Sebelas Maret University
Surakarta, Indonesia
nadaazizah.na@gmail.com

2nd Feri Adriyanto
Electrical Engineering Dept.
Sebelas Maret University
Surakarta, Indonesia
feri.adriyanto@staff.uns.ac.id

3rd Joko Slamet Saputro
Electrical Engineering Dept.
Sebelas Maret University
Surakarta, Indonesia
jssaputro89@ft.uns.ac.id

*Corresponding author: nadaazizah.na@gmail.com

Received: October 24, 2022; Accepted: November 28, 2022

Abstract—The development of technology at this time has an important role for all human needs and needs. One of the technologies that are currently developing is technology in the field of transportation. The development of electric vehicles is very relevant to be developed. However, in electric vehicles on the market, the control system used is less than optimal to respond to the load given to electric vehicles, resulting in a decrease in performance and waste of electrical energy. In general, BLDC motors which are often used as control systems use a position sensor (Hall effect sensor) in determining driver commutation. The use of position sensors often results in errors in configuration with the controller, difficulty in installation in case of damage, sensitivity of the sensor to temperature increases and the price of the sensor is relatively expensive. The use of sensorless method with Back EMF detection is an alternative solution to determine inverter commutation on BLDC motors. In this thesis, a BLDC motor speed control is developed which provides optimal, efficient and safe performance. This control system uses driver IC IR2101 and power switching MOSFET IFRZ44N. As a prototype, a 1000KV BLDC motor is used, controlled by an Arduino microcontroller and an ESP32 which is monitored by Blynk. The result achieved is that this system is able to control the rotation of the motor and stabilize the speed when there is a change in load. The efficiency of the no-load system reaches 46.48% and at maximum loading it reaches 36.98%, the best efficiency is obtained in the propeller II loading variation with an efficiency of 86.34%.

Keywords—Transportation, Electric vehicles, BLDC Motors, Efficiency

I. INTRODUCTION

The development of technology at this time has an important role for all human needs and needs. Among them are the needs in the field of information, transportation, communication or in other fields. Many technologies were created to help human work. With the development of technology, this does not only have a positive impact on human life, because the invention, creation, and development of technology brings humans in everything that is instant. One of the technologies that are currently developing is technology in the field of transportation. At this time the transportation system continues to be demanded to improve its quality and reliability in supporting community mobility.

There are more and more types of fuel oil transportation systems in Indonesian society. Based on data from the Central Statistics Agency, in 2017, the number of motorized vehicles in Indonesia was 138,556,669 units [1]. This causes the emission to increase following the increase in the number of vehicles and congestion that occurs in various regions. According to the Regulation of the State Minister for the Environment of the Republic of Indonesia Number 10 of 2012, exhaust gas emissions produced by motorized vehicles include carbon dioxide (CO₂), carbon monoxide (CO), nitrogen oxides (NO_x), hydrocarbons (HC), and oxygen (O₂) [2]. All of these exhaust gases are compounds that are harmful to the environment. * Corresponding Author. Tel: +62-812-28028845 E-mail: nadaazizah@student.uns.ac.id To overcome the pollution problem, an alternative transportation system is needed that is environmentally friendly, but still reliable to be used as a means of transportation. An alternative transportation system that is currently being developed is an electric vehicle, which is considered very effective and does not contribute to emissions for the environment. Electric vehicles use an electrical energy source that comes from a battery and is connected to an electronic control system that regulates the rotation of the electric motor so that it can operate. An electric motor is a device that is able to convert electrical energy into mechanical energy, where the conversion generally occurs through electromagnetic media [3]. One type of electric motor used as a driving force in electric vehicles is a brushless DC motor (Brushless Direct Current (BLDC)). BLDC motor is a DC motor that has the characteristics of large torque with small power [4]. This type of DC motor does not have brushes and commutators, so BLDC motors require little maintenance and can operate more quietly than other DC motors [5]. BLDC motors are divided into 2 types, namely sensed and sensorless. The difference between the two lies in the sensor used, where sensed BLDC uses a Hall effect sensor to monitor the rotor position. Meanwhile, the sensorless BLDC type does not use sensors to monitor the rotor position. However, it uses back EMF (Back Electromotive Force) detection. In general, BLDC motors that are often used use a position sensor (Hall effect sensor) in determining driver commutation. However, by using a position sensor, errors often occur during configuration with the controller, difficulty in installation in

case of damage, sensitivity of the sensor to temperature increases and the price of the sensor is relatively expensive [6]. From these problems, the use of a sensorless method that uses back EMF detection is an alternative solution to determine inverter commutation on BLDC motors. In order to operate, the BLDC motor requires a driver to be able to move and control the speed. Motor drivers generally consist of a collection of electronic components such as ICs, transistors and diodes. This motor driver is a circuit that modifies the DC voltage using the PWM method, resulting in a square/trapezoidal 3-phase DC voltage. Conventional BLDC motor drivers mostly use 6 inverter switches for electronic switching and back EMF detection to get the rotor position [7]. To be able to do the switching on the MOSFET. The BLDC motor driver circuit uses a MOSFET driver IC. One of them is IR2101. IR2101 is an IC that is used to control the MOSFET by providing a HIGH or LOW input to the MOSFET. This motor driver can operate with an input voltage between 0-20 V and is capable of turning on a MOSFET powered by a voltage of up to 600 V [8]. In its application, electric vehicles have several weaknesses, namely the development of technology in electric vehicles is not sustainable, each component is independent, both construction and design, charging supply is not optimal, requires a lot of batteries, speed is still low, and production costs are relatively expensive. In addition, the control system used in electric vehicles on the market is fixed, or cannot be reprogrammed. This causes the control system to be less than optimal, when electric vehicles are given a large load or extreme terrain conditions. The application of extreme loads and field conditions to electric vehicles will result in a decrease in the rotational speed of the BLDC motor, resulting in very large torque. The BLDC motor will respond by drawing high current from the inverter, to achieve steady state speed. This high current will cause a large energy consumption to the BLDC motor. Control systems on electric vehicles on the market generally provide a long enough response to reach steady state speed, resulting in wastage of battery consumption during the time to reach the steady state speed. Seeing the problems above, in this study a design was carried out to produce a BLDC motor speed control system in electric vehicles. The method used in this research is to design a BLDC motor driver. The control system that will be designed is a programmable control system, where the system can later be reprogrammed according to the terrain and loading conditions. The design of this system uses 2 microcontrollers, namely Arduino Nano as the brain of the speed control circuit and ESP32 as sensor readings as well as communication in sending monitoring data to the Blynk application. This circuit utilizes the IR2101 MOSFET driver IC to be NIGD to adjust the high/low switching on the MOSFET. NIGD receives HIGH/LOW input from the Arduino microcontroller which is then forwarded to the inverter. Control through the Arduino microcontroller is carried out using the PWM (Pulse Width Modulation) principle. The parameters of the system condition are monitored using the speed value reading and 3 sensors, namely the current sensor, voltage sensor and temperature sensor. The information data is then forwarded to the ESP32 microcontroller to be processed and sent to the Blynk application.

II. METHODS

A. BLDC Motor Speed Control System

The BLDC motor control system uses several electronic components that are arranged so that they can perform the switching process on the three motor phases alternately with accuracy. The control system is composed of several parts that are integrated with each other to produce a good control performance. The control system used in this system is a speed control system. In this system, the speed of the BLDC motor is regulated through the opening of the potentiometer. This value is processed into a PWM value by the microcontroller to be sent to the driver circuit as a regulator of the BLDC motor speed value.

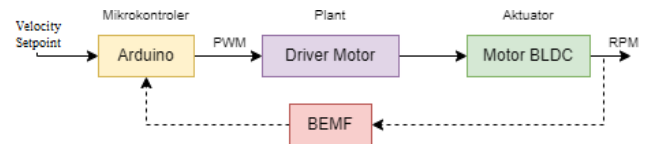


Fig 1. Open Loop Control System on BLDC motor

The Open Loop system is a control system whose output has no effect on the controlling action and there is no feedback to the microcontroller. In this type of control system, the motor speed value is purely regulated by a potentiometer without any feedback error to the microcontroller for processing. This system is quite simple and is usually applied to electric vehicles. This type of Open Loop system has a construction that is simple and easy to understand, but has several drawbacks such as less than optimal performance and decreased efficiency in extreme terrain conditions or overloading.

B. BLDC Motor Driver

The BLDC motor driver is a control circuit consisting of several electronic components that are integrated with each other to be able to perform the switching process on the MOSFET so that the BLDC motor can rotate properly. This circuit consists of a microcontroller, driver IC, MOSFET, and other supporting components. All components are integrated to be able to perform switching so that it can rotate the BLDC motor.

C. Design of BLDC Speed Control System

Control is done by providing a variation of the PWM signal to the driver circuit. The PWM value is taken from the potentiometer opening value which is converted to the PWM value.

This circuit uses several main components, including IC IR2101 and IRFZ44N mosfet. Three IR2101 motor driver circuits are arranged into a 3-phase motor driver circuit, by utilizing 6 IRFZ44N MOSFETs to perform switching on each phase based on information processing from Back-EMF. In the monitoring section, a current sensor module is used, a voltage divider circuit as a voltage sensor, a temperature sensor which is then connected to the ESP32 to be sent to the interface application created on Blynk. The figure below is a design of a BLDC motor speed control system.

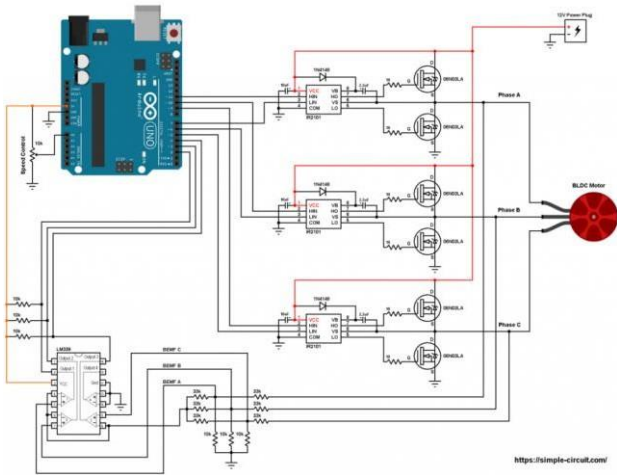


Fig 2. Design of BLDC Speed Control System

D. BLDC Motor

Brushless DC motor (BLDC) is a type of permanent magnet synchronous motor, which has a permanent magnet in the rotor and a trapezoidal back-electromotive force (EMF) [20]. The BLDC motor is supplied by a DC power source at the control, and requires a three-phase AC power source to drive the rotor parts of the motor. In contrast to conventional DC motors, this motor uses an electric commutation system or often called an electronically commutated motor. The BLDC motor has the characteristics of a DC engine by replacing the mechanical commutator and brush with a solid state switch and there is no electrical connection between the stator and the rotor [21]. Figure 3. shows the construction of a BLDC motor.

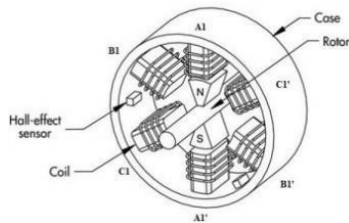


Fig 3. BLDC Motor

There are 2 types of BLDC motors, namely In- Runner Motors and Out-Runner Motors. As seen in Figure 4. the difference between the two lies in the location of the permanent magnet, where the In-Runner motor has a permanent magnet located inside the electromagnetic terminal, while the Out-Runner motor is located on the outside. These two types of BLDC motors have their respective characteristics as shown in the following table:

No	<i>In-Runner Motor</i>	<i>Out-Runner Motor</i>
1	High RPM, low torque	Low RPM, high torque
2	More efficient due to high rotation speed	Lower efficiency than In-Runner
3	Requires gearbox	No need for gearbox
4	A bit noisy	No sound

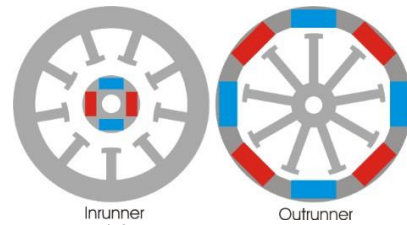


Fig 4. Inrunner Motor and Outrunner Motor

BLDC motors are widely used in various electronic components, especially in electric vehicles. This is because BLDC motors have various advantages compared to other motors, namely wide torque range, high speed, high efficiency, good dynamic response, strong, no slip, and others. BLDC motors are generally controlled using a 3-phase inverter, which requires a rotor position sensor element to start and supply the commutator sequence to then control the inverter.

E. Three Phase Motor Power Efficiency

Efficiency is defined as a measure of the efficiency of the motor to convert electrical energy into mechanical energy, which is expressed as a ratio / ratio of output power to input power. The NEMA definition of energy efficiency is that efficiency is the ratio or ratio of useful output power to total input power, expressed as a percentage. Usually also expressed by the ratio of input and output power to loss.

$$(1)$$

η = Efficiency (%)

P_{out} = The output power of an induction motor (Watt)

P_{in} = Induction motor input power (Watt)

F. Back EMF (Back Electromotive Force)

An emf voltage is generated when a wire moves through a magnetic field. As the rotor rotates, a back EMF waveform is generated from each coil winding, which can be used for position detection typically applied to pumps, fans and similar applications with low torque variations at startup and normal operation. In practice, a 60° window will be applied to the face coil which is not actuated

and the comparator is used to detect the zero crossing which is equivalent to a signal change in the Hall sensor one of the coils is given positive energy the other is negative energy, after that the comparator can compare the Back EMF of the open coil to have a DC bus voltage after detecting the zero crossing, it will index the sequence energizing to the next step [27]. At the time of the trapezoidal wave, the Back EMF motor will change the polarity and amplitude as it rotates, because the Back EMF is proportional to the speed, so the waveform will have low amplitude at startup and slow speed, making it difficult to detect zero crossing.

So the solution, the motor rotates in open loop mode (open loop) until the speed produces sufficient Back EMF for measurement. The emergence of EMF depends on the strength of the magnetic flux line, the number of turns of the conductor, the angle of intersection of the magnetic flux with the conductor, and the speed at which the conductor cuts the magnetic flux line. There is no induced current that

occurs in the dynamo conductor, if the armature or generator is stationary (not rotating).

At the time of the motor startup process, a startup detection process is needed on the motor, namely IPD detection. IPD is used to detect the initial position when the motor is stationary. Rotor align aligns the rotor to a known position, before starting to switch, often causing reverse rotation at startup.

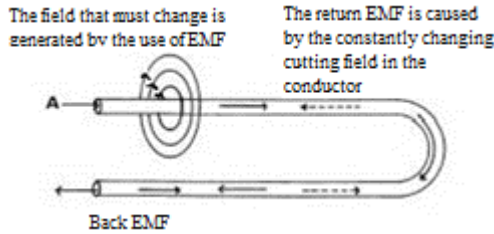


Fig 5. Back EMF Illustration

III. RESULTS AND DISCUSSIONS

A. Simulation experiment

Simulation testing is done using Proteus software. The tests carried out at this stage are only limited to testing the PWM waveform reading and the output waveform from the driver circuit, then testing the voltage on the phase and input current of the circuit. Observation of the output waveform is carried out to determine the waveform in each phase which will be compared with the output waveform from the hardware. The simulation results that have been carried out can be seen in the following image

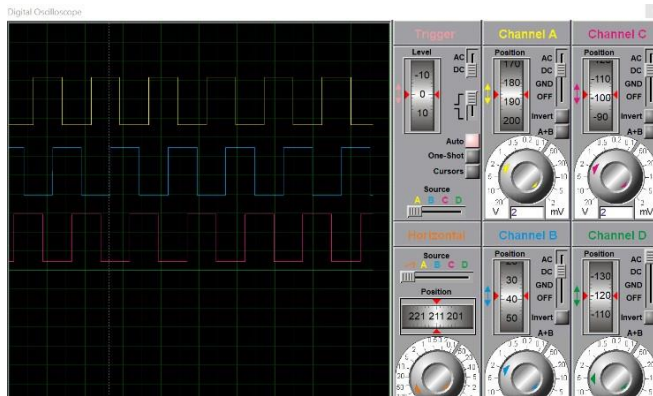


Fig 6. Driver Output Simulation Test Graph

B. Design Tool

This stage is simulated by creating a simulation circuit on Proteus, after the simulation circuit is complete, it is continued by making a PCB layout based on the circuit that has been made in Eagle. After the PCB layout is finished, check the path and then print it to the PCB board. Then the component assembly is carried out using solder. The results of making the tool can be observed in Figure 4.3. The schematic circuit is then converted into a PCB layout using Eagle. The arrangement of components is made as neat as possible with the appropriate path and minimizes the presence of jumper cables. The PCB board design uses a single sided layer with a size of 15.5 x 12 cm. The components used in this circuit are DIP components.

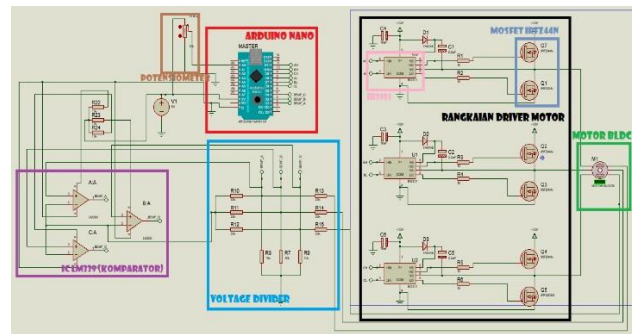


Fig 7. Design Tool (Master) on Proteus

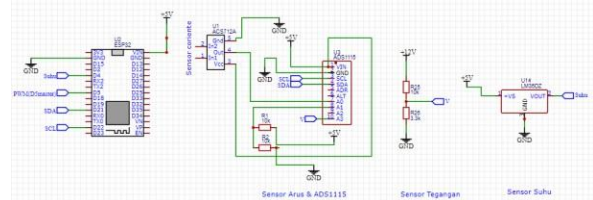


Fig 8. Design Tool (Slave) on Easyeda

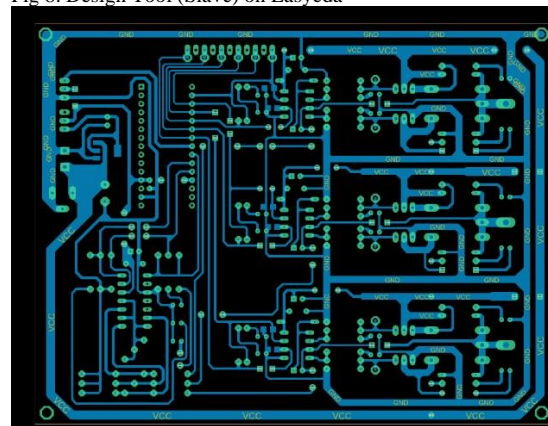


Fig 9. Layout PCB (Master)

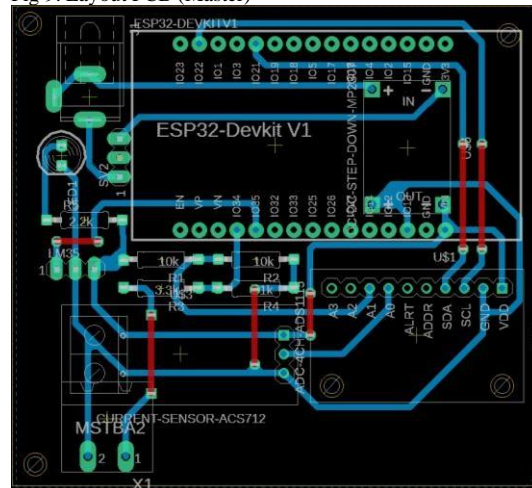


Fig 10. Layout PCB (Slave)

C. Hardware Implementation

The next step is to try it in the real hardware situation, in this testing we use 2 different color landing pad with 2 different testing area, which is in the grass field and asphalt field.

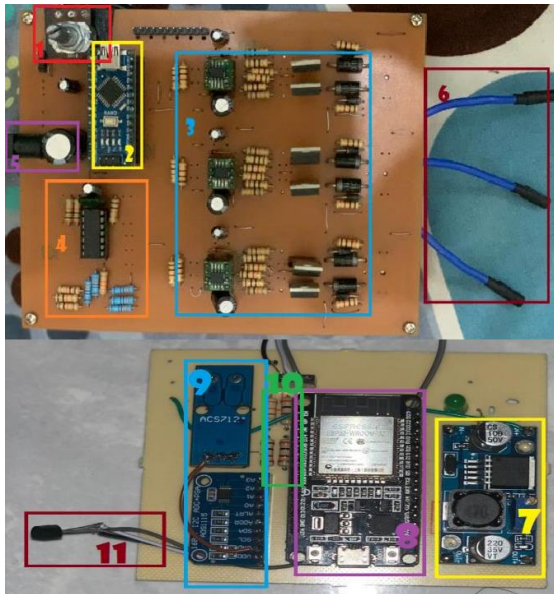


Fig 13. DIY ESC

As shown in figure 13, hardware is a combination of the Arduino Nano microcontroller, a 3-phase mosfet driver circuit, as well as several circuits for the monitoring system. it can be observed that the hardware is composed of components according to the design made.

The following is a description of the hardware circuit that has been made:

1. Potensiometer 10k
2. Arduino Nano
3. Driver motor BLDC
4. IC LM339 and Voltage Divider
5. Port input Supply Voltage
6. Port output 3-phase
7. Stepdown LM39
8. ESP32
9. Sensor ACS712 and ADS1115
10. Voltage Sensor
11. LM35 Sensor



Fig 14 Load Variation

1. PWM Value Reading Test
 - a. PWM Wave

The test is carried out to determine the signal generated on the three Arduino Nano PWM pins that enter the driver circuit. The PWM signal from the microcontroller will regulate the switching in each phase so that the motor rotational speed can be adjusted. In this test a sample of the PWM value of 50 is taken where the motor rotates at a speed

of 2456 rpm, then observed using an oscilloscope as shown in Figure 14. In this condition, the voltage that flows to the motor is 6.34V and the current is 0.25A. The resulting PWM signal corresponds to the reference, where there is a 120° difference between the phases. The voltage level of the PWM is HIGH for 5V and LOW for 0V.

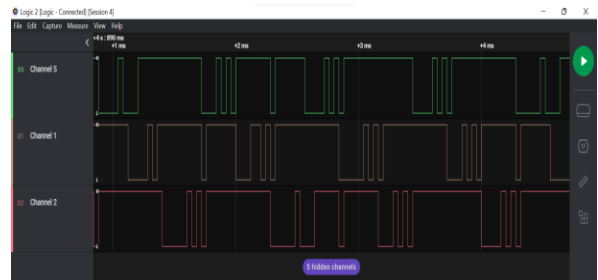


Fig 15 PWM Wave

b. No-Load ABC Phase Output Waveform

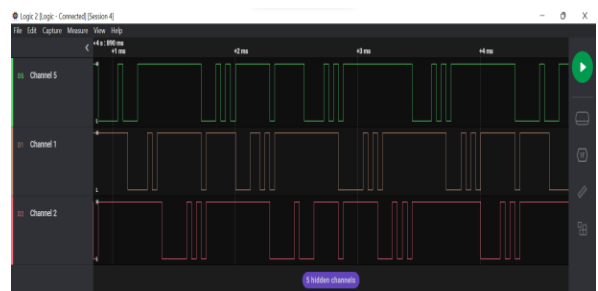


Fig 16. No-Load ABC Phase Output Waveform

TABLE I. NO-LOAD DRIVER MEASUREMENT

PWM	Duty Cycle	Voltage (V)	Current (A)	Frequency (kHz)	RPM
50	25%	5,7	0,25	6,25	2456

c. Phase Output Waveform ABC Propeller Load (I)

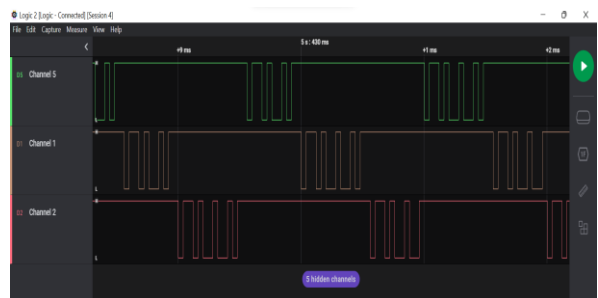


Fig 17. Phase Output Waveform ABC Propeller Load (I)

TABLE II. PROPELLER LOAD (I) DRIVER MEASUREMENT

PWM	Duty Cycle	Voltage (V)	Current (A)	Frequency (kHz)	RPM
50	66,67%	5,91	0,52	8,33	2894

d. Phase Output Waveform ABC Propeller Load (II)

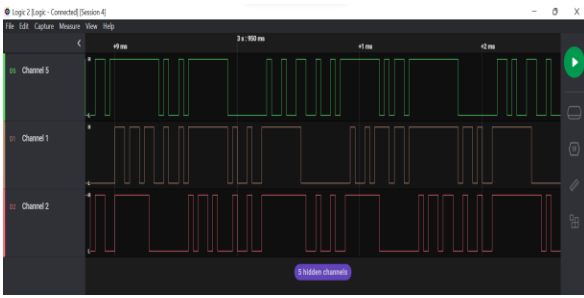


Fig 18. Phase Output Waveform ABC Propeller Load (II)

TABLE III. PROPELLER LOAD (II) DRIVER MEASUREMENT

PWM	Duty Cycle	Voltage (V)	Current (A)	Frequency (kHz)	RPM
50	33,33%	6,12	0,83	8,33	3588

e. Phase Output Waveform ABC Propeller Load (III)

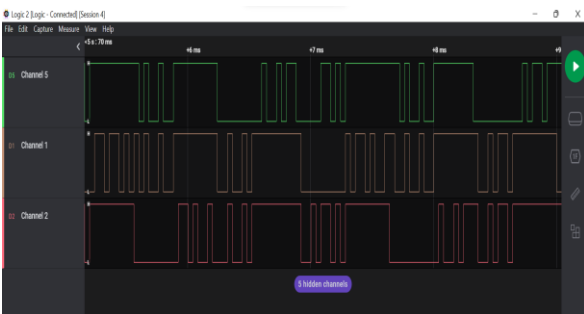


Fig 19. Phase Output Waveform ABC Propeller Load (III)

TABLE IV. PROPELLER LOAD (III) DRIVER MEASUREMENT

PWM	Duty Cycle	Voltage (V)	Current (A)	Frequency (kHz)	RPM
50	33,33%	6,48	2,18	8,33	3986

2. PWM Value Reading Test

a. PWM Value Reading Results

The reading of the PWM value is carried out through observations on the Arduino serial monitor, where the potentiometer value is changed so that the value of the resulting PWM also changes. Changes in the potentiometer will produce a varying voltage with a range of 0V to 5V which is forwarded to port A0 on the Arduino. The input value read from the port is then processed into a PWM value with a range from 0 to 255.

Table 5. PWM response to changes in potentiometer opening

Potentiometer Ratio	PWM Value
0	0
10	27
20	52
30	78
40	103
50	130
60	155
70	179
80	205
90	232
100	255

3. Testing Current Sensors, Connection Sensors, and Temperature Sensors

Testing this sensor is done by reading the output value of the current, voltage, and temperature sensors in the circuit. The sensor connected to the ADS1115, serves as a substitute for the digital analog converter on the ESP32. By forwarding through the SCL and SDA ports on the ESP32, further calibration is carried out to adjust sensor measurements by adding regression calculations in each sensor calibration.

TABLE V. CURRENT, CONNECTION, AND TEMPERATURE SENSOR TEST RESULTS

Potentiometer Ratio	PWM Value	Voltage A (V)	Voltage B (V)	Voltage C (V)	Current (A)	Temperature (C)
0	0	0	0	0	0	30,34
10	27	5,52	5,36	5,78	0,28	35,36
20	52	6,34	6,27	6,22	0,35	37,91
30	78	6,83	6,61	6,75	0,39	38,12
40	103	7,45	7,29	7,18	0,41	39,04
50	130	7,78	7,64	7,82	0,45	39,61
60	155	8,26	8,03	8,15	0,49	39,35
70	179	8,42	8,37	8,29	0,52	38,1
80	205	8,76	8,92	8,64	0,56	37,6
90	232	9,16	9,27	9,36	0,61	37,2
100	255	10,08	9,96	10,12	0,65	37,14

Fig 21. Current, Voltage, and Temperature Sensor Test Results

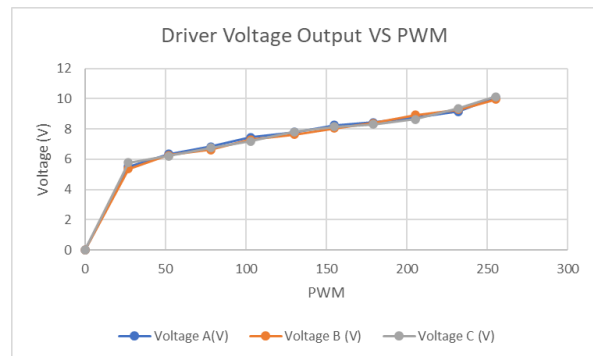


Fig 22. PWM value and Phase Voltage

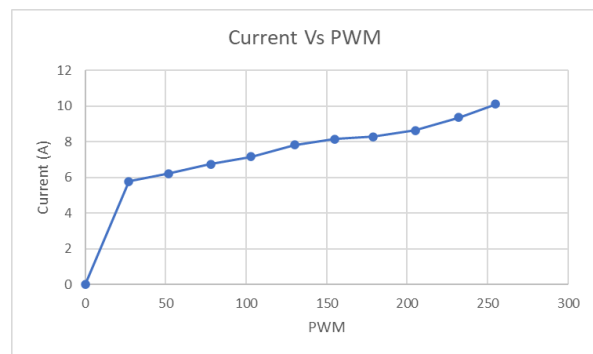


Fig 23. PWM Value and Input Current

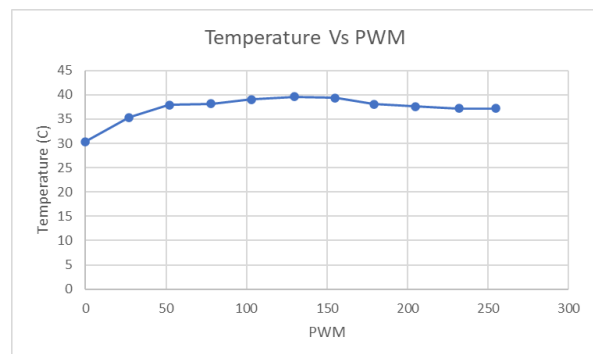


Fig 24. PWM Value and Temperature

4. BLDC Motor Speed Reading Test

The reading of the motor speed value is carried out using an infrared sensor on the motor rotation. The speed value is sought by recording the rpm in each PWM value in 10% increments and a regression equation value is made from the speed. The reading of the regression results is then processed by the microcontroller to be displayed as an RPM value on the Arduino serial monitor.

TABLE VI. PWM VALUE CHANGES TO MOTOR ROTATIONAL SPEED

Potentiometer (%)	PWM	No Load (rpm)
0	0	0
10	27	1328
20	52	2558
30	78	3887
40	103	5019
50	130	6397
60	155	7528
70	179	8906
80	205	10087
90	232	11416
100	255	12548

TABLE VII. ERROR PERCENTAGE OF MOTOR RPM

Potentiometer (%)	PWM	Original RPMs	Arduino RPM	% Error
0	0	0	0	0
10	27	1459	1328	8,978
20	52	2469	2558	3,64
30	78	3672	3887	5,855
40	103	4695	5019	6,9
50	130	1641	6397	4,168
60	155	7354	7528	2,366
70	179	8656	8906	2,888
80	205	10327	10087	2,325
90	232	11198	11416	1,946
100	255	12827	12548	2,175

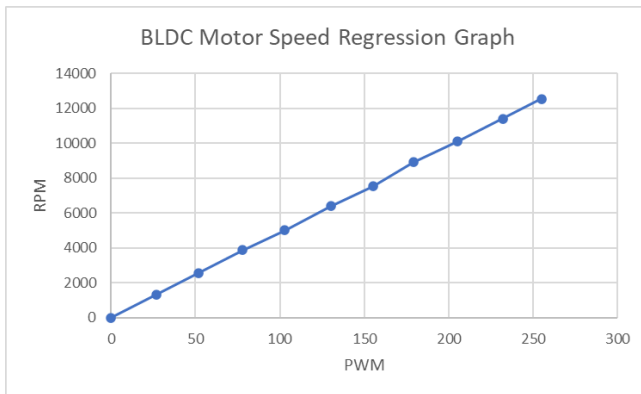


Fig 25. BLDC Motor Speed Regression Graph

The results of the BLDC motor rotation speed test above are then processed into a regression graph as shown in Figure 25 to find out the equations of the tools made. From the graph it can be seen that the increase in the motor rotation speed is quite stable. So that the regression equation can be seen as follows:

$$y = 49.224x - 2.4765$$

The regression equation above is an equation that shows the relationship between the PWM value and the motor rotational speed value. X is the PWM value and Y is the

rotating speed value. From these equations it can be used to find the value of the motor speed at a certain PWM

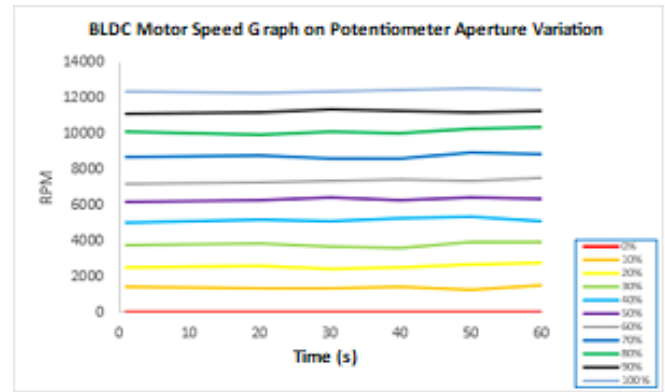


Fig 26. Speed tracking on BLDC motors This test is carried out to determine the level

of precision of the motor rotation to the given PWM value. The PWM value is given through the potentiometer opening from 0% to 100%. Readings were carried out on each variation for 1 minute and resulted in 66 data to be processed and compared.

5. Testing of Load Variations on BLDC Motors

The test is carried out by adding a load variation in the form of no load and using a load in the form of a propeller with 3 types of sizes. Propeller I with a length of 8 inches and a pitch of 4 inches. Propeller II with a length of 9 inches and a pitch of 5 inches. Propeller III with a length of 10 inches and a pitch of 6 inches

a. No-load Driver Test

The test was carried out 4 times by changing the PWM value in each experiment. The resulting RPM value continues to increase according to the rotation of the motor.

Table 9. No-load Driver Testing

PWM	RPM	Voltage A(V)	Voltage B (V)	Voltage C (V)	Driver Current (A)	Driver Current (B)	Temperature (C)
50	2456	5,7	5,7	5,7	0,48	0,25	33,19
75	3749	6,3	6,3	6,3	0,75	0,37	36,71
100	4863	7,4	7,4	7,4	0,82	0,42	38,13
130	6233	8,2	8,2	8,2	0,91	0,49	38,38

b. Driver Testing on Propeller Load (I)

In testing the loading using propeller I, it is done by adding a load in the form of a propeller of 80x40 size to the motor to determine the response given by the motor.

TABLE VIII. DRIVER TESTING WITH PROPELLER LOAD (I)

PWM	RPM	Voltage A(V)	Voltage B (V)	Voltage C (V)	Driver Current (A)	Driver Current (B)	Temperature (C)
50	2894	5,91	5,91	5,91	0,61	0,52	36,87
75	5465	6,68	6,68	6,68	0,85	0,81	39,18
100	6299	7,25	7,25	7,25	1,6	1,3	40,41
130	7388	7,79	7,79	7,79	2,1	1,8	38,75

c. Driver Testing on Propeller Load (II) The test is carried out by providing a propeller

II load, adding a load in the form of a 90x60 propeller to the motor to determine the response given by the motor.

TABLE IX. DRIVER TESTING WITH PROPELLER LOAD (II)

PWM	RPM	Voltage A(V)	Voltage B (V)	Voltage C (V)	Driver Current (A)	Driver Current (B)	Temperature (C)
50	3588	6,12	6,12	6,12	0,9	0,8	39,42
75	4543	6,75	6,75	6,75	1,8	1,6	40,05
100	5343	7,34	7,34	7,34	2,5	2,4	39,21
130	6487	7,86	7,86	7,86	3,8	3,2	38,32

d. Driver Testing on Propeller Loading III The test is carried out by providing a propeller III load, adding a load in the form of a 10x60 propeller to the motor to determine the response given by the motor.

TABLE X. DRIVER TESTING WITH PROPELLER LOAD (III)

PWM	RPM	Voltage A(V)	Voltage B (V)	Voltage C (V)	Driver Current (A)	Driver Current (B)	Temperature (C)
50	3986	6,48	6,48	6,48	3,54	2,18	29,95
75	4985	7,15	7,15	7,15	5,0	4,61	27,22
100	0	0	0	0	0	0	0
130	0	0	0	0	0	0	0

In this variation of loading, the current is very large, so it cannot continue the testing process in PWM 100 and 130. This is because the circuit cannot work at currents above 5A, so that it goes above 5A, the cut off system causes the system to shut down immediately and cannot perform measurement process again.

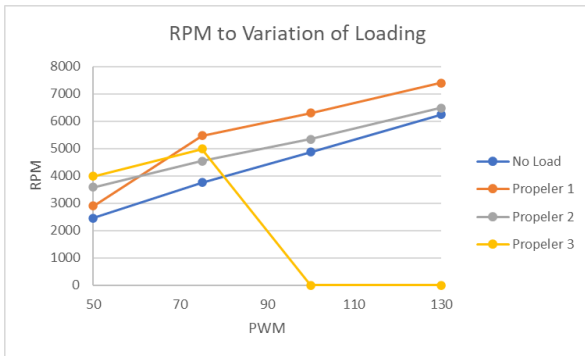


Fig 27. Comparison Graph of Speed Response on Variation of Loading

6. Blynk Monitoring Test

Testing the monitoring system of the Blynk application displayed on a smartphone. Testing is done by providing sample data from the monitoring system from several existing sensors. On Blynk will display PWM data, current, supply voltage, and temperature. The read delay of the Blynk application is set to 1 second to keep the data transmission of the ESP32 stable.

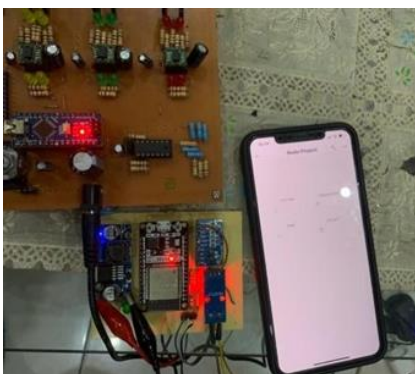


Fig 28. Motor Control System with Monitoring Blynk

7. System Efficiency Analysis

This analysis was carried out to determine the performance of the BLDC motor driver under no-load conditions and conditions with variations in loading.

a. Calculation of 50 PWM System Efficiency

TABLE XI. SYSTEM EFFICIENCY ANALYSIS TABLE ON PWM 50

Condition	Driver			Motor			Efisiensi (%)
	V	I	P	V	I	P	
No Load	6.68	0.75	5.01	6	0.37	2.22	44,31%
Propeller I	6.75	0.85	5.7375	6.28	0.81	5.0868	88,65%
Propeller II	6.81	1.78	12.1218	6.58	1.6	10.528	86,85%
Propeller III	7.15	5	35.75	6.89	4.61	31.7629	88,84%

b. Calculation of 75 PWM System Efficiency

TABLE XII. SYSTEM EFFICIENCY ANALYSIS TABLE ON PWM 75

Condition	Driver			Motor			Efisiensi (%)
	V	I	P	V	I	P	
No Load	6.68	0.75	5.01	6	0.37	2.22	44,31%
Propeller I	6.75	0.85	5.7375	6.28	0.81	5.0868	88,65%
Propeller II	6.81	1.78	12.1218	6.58	1.6	10.528	86,85%
Propeller III	7.15	5	35.75	6.89	4.61	31.7629	88,84%

c. Calculation of 100 PWM System Efficiency

TABLE XIII. SYSTEM EFFICIENCY ANALYSIS TABLE ON PWM 100

Condition	Driver			Motor			Efisiensi (%)
	V	I	P	V	I	P	
No Load	7.25	0.82	5.945	6.57	0.42	2.7594	46,41%
Propeller I	7.34	1.6	11.744	6.87	1.3	8.931	76,04%
Propeller II	7.42	2.5	18.55	7.19	2.4	17.256	93,02%
Propeller III	0	0	0	0	0	0	0%

d. Calculation of 130 PWM System Efficiency

TABLE XIV. SYSTEM EFFICIENCY ANALYSIS TABLE ON PWM 130

Condition	Driver			Motor			Efisiensi (%)
	V	I	P	V	I	P	
No Load	7.79	0.91	7.0889	7.11	0.49	3.4839	49,14%
Propeller I	7.86	2.1	16.506	7.39	1.8	13.302	80,58%
Propeller II	7.94	3.8	30.172	7.71	3.2	24.672	81,77%
Propeller III	0	0	0	0	0	0	0%

e. Calculation of Average Efficiency from Changes in PWM

TABLE XV. TABLE OF AVERAGE EFFICIENCY OF PWM CHANGE

Condition	Efisiensi				Average Efisiensi
	50	75	100	130	
No Load	46,09%	44,31%	46,41%	49,14%	46,48%
Propeller I	78,69%	88,65%	76,04%	80,58%	81%
Propeller II	83,75%	86,85%	93,02%	81,77%	86,34%
Propeller III	59,11%	88,84%	0%	0%	36,98%

The results of the efficiency calculations show different values in each variation of loading, given the many test errors, both from the quality of the components used and the readings from the sensor which are less accurate due to the



very fast switching of the motor. It can be seen that to be able to operate a BLDC motor, the motor driver consumes 2.8 W of power at no-load conditions and 22.9 W at the largest loading condition, namely the 10x60 propeller. The efficiency of this circuit is quite good where the load variation of the propeller I is 81% and the variation of the loading of the propeller II is 86.34%. This test obtained good results where the motor can rotate with relatively small power consumption and has a fairly stable speed value.

IV. CONCLUSION

From the results of the experiment and discussion above, it can be concluded:

1. A BLDC motor speed control system has been successfully developed using the Back EMF method which provides optimal and safe performance, using a BLDC motor and monitored by the Blynk application.
2. The performance of the system is indicated by the efficiency results obtained from each load variation. The power efficiency of the no-load system reaches 46.48%, while at maximum loading it reaches 36.98%. The best efficiency is obtained in the propeller II loading variation with an efficiency of 86.34%.

ACKNOWLEDGMENT

The authors express their gratitude to this chance to all the people that has helped to write and execute this experiment.

REFERENCES

- [1] Badan Pusat Statistik. 2017. Perkembangan Jumlah Kendaraan Bermotor Menurut Jenis, 1949-2017. BPS Indonesia. Jakarta.
- [2] Syamsudin, A. 2012. Peraturan Menteri Negara Lingkungan Hidup Republik Indonesia Nomor 10 Tahun 2012. Berita Negara Republik Indonesia. No.788 (Revisi 2018).
- [3] John Prabu, M., Poongodi, P., & Premkumar, K. "Fuzzy supervised online coactive neuro-fuzzy inference system-based rotor position control of brushless DC motor. IET Power Electronics" IET Power Electronics, vol. 9, pp. 2229–2239, June. 2016.
- [4] F. E. Nugroho. "Perancangan sistem informasi penjualan online studi kasus tokoku." Jurnal Teknik Mesin, Elektro dan Ilmu Komputer, vol. 7, pp. 717-724, Nov. 2016.
- [5] M. S. Aspalli, F. M. Munshi and S. L. Medegar, "Speed control of BLDC motor with Four Switch Three Phase Inverter using Digital Signal Controller," 2015 International Conference on Power and Advanced Control Engineering (ICPACE), Bengaluru, India, 2015, pp. 371-376, doi: 10.1109/ICPACE.2015.7274975.
- [6] Q., Sadli, M., & Bintoro, A. "Penggunaan motor dc brushless sunny sky x2212-13 kv: 980 ii pada perancangan quadcopter." Jurnal Energi Elektrik, vol. 7, pp. 39-46, 2018.
- [7] Ebadpour, M., Sharifian, M. B. B., & Babaei, E. "Modeling and synchronized control of dual parallel brushless direct current motors with single inverter." Computers & Electrical Engineering, vol. 70, pp. 229-242, 2017.
- [8] Rashid, M.H. 2004. Power Electronics Circuit, Devices, And Applications 3rd Edition, Pearson Education Inc, University of West Florida
- [9] Braco Sola, E. (2016). Design and simulation of a single-phase inverter with digital PWM.
- [10] M. Adamski. "Analysis of propulsion systems of unmanned aerial vehicles." Journal of Marine Engineering & Technology, vol. 16, pp. 291-297, Oct. 2017.
- [11] Sivakami, R., & Sugumar, G. "Speed control of sensorless brushless DC motor by computing back emf from line voltage difference." Jurnal Teknik Mesin, Elektro dan Ilmu Komputer, vol. 10, pp. 31-738, Jun. 2020.
- [12] Sartika, E. M., Muliady, M., Sarjono, R., & Yuvens, V. "Pengontrolan Kecepatan Rotor BLDC UAV Berdasarkan Hasil Identifikasi menggunakan Metode Regresi." Jurnal Teknik Energi Elektrik, Teknik Telekomunikasi, & Teknik Elektronika, vol. 9, pp. 114, Jan. 2021.
- [13] S. Wanto. E. Purwanto. & O. A. Qudsi. "Peredaman Noise pada Deteksi BEMF Motor BLDC Sensorless Menggunakan Digital Filter." INOVTEK-Seri Elektro, vol. 3, pp. 123-132, Des. 2021.
- [14] Ahmad, M. (2020). Rancang bangun kendali dan monitoring pada kecepatan motor bldc dengan sensor hall.
- [15] Affandy, J. T. (2019). Desain Inverter Satu Fasa dengan Monitoring Daya Menggunakan Arduino.
- [16] Braco Sola, E. (2016). Design and simulation of a single-phase inverter with digital PWM.
- [17] International Rectifier, "IRFZ44N Datasheet," Accessed: May. 20, 2022.[Online]. Available: <https://www.alldatasheet.com/datasheetpdf/pdf/68131/IRF/IRFZ44N.html>
- [18] International Rectifier, "IR2101 Datasheet," Accessed: May. 20, 2022. [Online]. Available: <https://www.alldatasheet.com/datasheetpdf/pdf/68056/IRF/IR2101.html>
- [19] Regulator Tegangan, "MP1584 Datasheet," Accessed: May. 20, 2022. [Online]. Available: <https://www.alldatasheet.com/datasheetpdf/pdf/551592/MPS/MP1584.html>
- [20] E. Afjei, A. Nadian Ghomsheh and A. Karami, "Sensorless speed/position control of brushed DC motor," 2007 International Aegean Conference on Electrical Machines and Power Electronics, Bodrum, Turkey, 2007, pp. 730-732, doi: 10.1109/ACEMP.2007.4510598.
- [21] R. B. Ashok, & B. M. Kumar. "Comparative Analysis of BLDC motor for different control topology." Energy Procedia, vol. 117, pp. 314-320, Jun. 2017.
- [22] PWM, Accessed: April. 20, 2022. [Online]. Available: <https://arduino.cc/en/tutorial/PWM>
- [23] P. Deshpande, S. S. Mopari and P. S. Swami, "Power factor correction and power quality improvement in BLDC motor drive using SEPIC converter," 2019 IEEE International Conference on Electrical, Computer and Communication Technologies (ICECCT), Coimbatore, India, 2019, pp. 1-4, doi: 10.1109/ICECCT.2019.8868964.
- [24] Hendershot, J. R., & Miller, T. J. (1994). Design of brushless permanent- magnet motors.
- [25] I. Efendi, "it-jurnal.com," Accessed: May. 20, 2022. [Online]. Available: <https://www.itjurnal.com/pengertian-dan-kelebihan-rduino/>
- [26] Arduino, [Online]. Available: <https://store.arduino.cc/usa/arduino>. [Diakses 20 April 2022]
- [27] Back EMF, Accessed: May. 21, 2022. [Online]. Available: <https://circuitglobe.com/what-is-back-emf-in-dc-motor.html>
- [28] Back EMF, Accessed: May. 21, 2022. [Online]. Available [https://elektronika-dasar.web.id/electromotive-force-emf-gaya- gerak-listrik/](https://elektronika-dasar.web.id/electromotive-force-emf-gaya-gerak-listrik/)
- [29] ACS712 Datasheet, 2006, Allegro MicroSystems Inc., Worcester, Massachusetts, USA. Blynk, Accessed: June. 20, 2022. [Online]. Available: <https://blynk.io>
- [30] Blynk, Accessed: June. 20, 2022. [Online]. Available: <https://blynk.io>
- [31] ADS1115, "ADS1115 Datasheet," Accessed: June. 20, 2022. [Online]. available: <https://www.alldatasheet.com/datasheetpdf/pdf/292735/TI/ADS1115.html>
- [32] Muliadi, M., Imran, A., & Rasul, M. (2020). Pengembangan tempat sampah pintar menggunakan esp32. Jurnal Media Elektrik, 17(2), 73-79.
- [33] LM35, "LM35 Datasheet," Accessed: June. 20, 2022. [Online]. Available: <https://www.alldatasheet.com/datasheet-pdf/pdf/517588/TI/LM35.html>
- [34] E. E. Prasetyo, & W. F. Arum. "Analisis Perbandingan Kinerja Brushless Motor Menggunakan Metode Eksperimen." Jurnal Nasional Teknik Elektro dan Teknologi Informasi, vol. 10, pp. 71-76, Feb. 202

